

Effect of Sn Doping on Structural and Optical Properties of 2D α -MoO₃ Nanostructures

Amin Eftekhari¹, Mohammad Bagher Rahmani^{1,*}, Fatemeh Masdarolomoor²

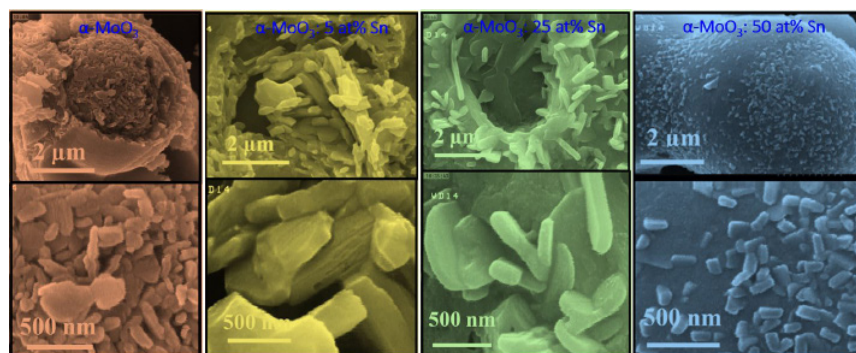
¹Department of Physics, Shahrood University of Technology, Shahrood, Iran

²Department of Chemistry, Shahrood University of Technology, Shahrood, Iran

HIGHLIGHTS

- The simple and low cost method of spray pyrolysis was utilized to synthesize 2D α -MoO₃ thin films.
- Sn doped MoO₃ thin films with different amounts of impurity were deposited with success
- Undoped and Tin doped MoO₃ thin films were characterized structurally and optically using various techniques.

GRAPHICAL ABSTRACT



ABSTRACT

Undoped and tin (Sn) doped molybdenum trioxide (α -MoO₃) nanostructured thin films (which has lamellar (2D) structure) have been prepared using a simple and cost effective technique of spray pyrolysis on glass substrates at 450°C. Surface morphology, optical and structural properties of samples have been investigated using FESEM, UV-Vis spectroscopy and XRD analysis techniques, respectively. FESEM images showed the formation of some discrete micro-spheres on the surface, which with the increasing in the amount of dopant homogenous and dense nano-platelets was grown on top of these micro-spheres. The XRD pattern analysis shows that all samples have been grown in orthorhombic (α -MoO₃) crystal structure and except for the sample doped with 50 at% Sn which had a weak peak of SnO₂, no peak have been observed corresponding to the incorporation of Sn. By increasing the amount of impurity, optical transmittance of samples were increased from ~27 to 50%. Also, the band gap of samples were calculated using transmission data. An increasing of band gap from 3.34 to 3.89 eV was observed with increasing in the amount of doping.

ARTICLE INFO

Article history:

Received 17 November 2016

Received in revised form

15 December 2016

Accepted 26 February 2017

Keywords:

Crystal structure
Molybdenum trioxide
Micro-spheres
Nano-platelets
Spray pyrolysis

* Corresponding author. Tel. & fax: +982332395270

E-mail address: mbrahimani@shahroodut.ac.ir ; mbrahimani@yahoo.com

1. Introduction

In the past decade, nanostructures of metal oxides have attracted the attention of many scientists. These structures have inimitable electrical, optical, magnetic and catalytic properties [1]. Among them, molybdenum trioxide (MoO_3), recently due to the fascinating properties and applications of nanostructures on large areas are taken into consideration [2]. Because of its layered structure, MoO_3 has been recently focused due to its electrochromic and photochromic properties, which makes it a good candidate for use in important applications such as smart windows and display devices [3]. MoO_3 is a n-type semiconductor with a wide band gap of about 2.9–3.5 eV and due to these mentioned properties its applications as catalyzers, gas sensors and solar cells have been reported [4, 5]. Generally MoO_3 has three forms: the well-known thermodynamically stable orthorhombic α - MoO_3 , metastable monoclinic β - MoO_3 , and hexagonal h- MoO_3 . Between these three forms, α - MoO_3 has attracted most interests because of its diverse properties as in supercapacitors [6]. Using different techniques for growing thin films of this material leads to diverse morphologies and structures and hence to distinct properties. Thin films preparation of MoO_3 have been reported by different deposition techniques such as thermal evaporation [4], spray pyrolysis [5, 7], hydrothermal [8], physical vapor deposition [1], sol-gel [9], spin coating [10], sputtering [11] and electron beam evaporation [12]. Among these techniques spray pyrolysis has attracted researchers' attention because it's a simple and cost effective method. Also, it can be implemented for depositing thin films on large areas. However, it is involved with a large number of interrelated variables like flow rate, carrier gas pressure, distance between the substrate and spraying nozzle and etc., which are all to be optimized to obtain a thin film with the desired quality [13]. Control of growth parameters with aiming to achieve well-defined nanostructured morphologies and also, doping with a metal or metal oxide impurities may open new opportunities for exploring exclusive physical and chemical properties and more potential uses [14-17]. There are several reports on doping of MoO_3 with different elements as impurities. M. Kovendhan *et al.* have deposited undoped and lithium (Li) (1–5 wt%) doped MoO_3 thin films on ITO coated glass substrates using spray pyrolysis at a substrate temperature of 325 °C. In their report, Li doping has induced modifications in physical and

chemical properties of their samples [13]. Niobium (Nb) doped molybdenum trioxide (MoO_3) thin films have been synthesized using spray pyrolysis deposition technique, by S.S. Mahajan *et al.* [18]. Their report indicates that by increasing the dopant concentration, the structure of MoO_3 undergoes a phase transformation from orthorhombic to amorphous. In another case, J. Kaur *et al.* have studied the properties of SnO_2 thin films prepared by a sol-gel spin coating process using different percentages (1, 5, 10 and 20 wt. %) of MoO_3 as impurity on glass substrates. They have observed that with an increase in doping concentration the reflectance decreases because of an increase in roughness and a decrease in the number of free electrons [19].

In this paper, we have studied the effect of Sn doping (Sn/Mo atomic ratio = 0.05, 0.10, 0.15, 0.25, 0.50 in precursor solution) on structural and optical properties and surface morphology of MoO_3 thin films on glass substrate prepared using the simple route of spray pyrolysis. The importance of the work that has been done in this manuscript is due to the fabrication of Sn doped 2D α - MoO_3 nano-platelets using the simple and low cost technique of spray pyrolysis. Two-dimensional (2D) materials can show unique electronic and optical properties when the number of planes are reduced, due to changes in the electronic band structure. Recently, fabrication of biosensors and high-performance field effect transistors have been reported using 2D nature of α - MoO_3 [20-22].

2. Experimental

2.1. Materials and methods

In order to deposition of thin films, firstly, glass substrates were washed by deionized water and soap, then substrates ultrasonically cleaned in a mixture of acetone and ethanol. Finally, the substrates were washed with deionized water and dried with a mild stream of clean and dry air.

For synthesis of undoped and Sn doped MoO_3 thin films, ammonium molybdate tetrahydrate ($(\text{NH}_4)_6\text{Mo}_7\text{O}_{24}\cdot 4\text{H}_2\text{O}$ extra pure (Merck)) was utilized as starting material and deionized water as solvent. Tin (II) chloride dehydrate ($\text{SnCl}_2\cdot 2\text{H}_2\text{O}$ (Merck)) was taken as the source of impurity. In order to prepare spray solution, firstly, 3.089 gr of $(\text{NH}_4)_6\text{Mo}_7\text{O}_{24}\cdot 4\text{H}_2\text{O}$ was dissolved in 20 mL deionized water and different amounts of $\text{SnCl}_2\cdot 2\text{H}_2\text{O}$ (Sn/Mo atomic ratio = 0.05, 0.10, 0.15, 0.25, 0.50 in precursor solution) were dissolved in 30 ml deionized

water and ethanol (1:1 ratio) by magnetic stirring. Then prepared solutions were stirred using a magnetic stirring heater at 40 °C for 2 hours until a clear and absolutely transparent solutions were obtained. Lastly, the obtained solutions were sprayed on top of glass substrates. Deposition parameters for spraying all samples were controlled as following: Substrate temperature: 450 °C, Nozzle to spray distance: 35cm, Dry and clean air pressure: 2 mbar, Precursor solution spray rate: 5 mL/min. Also, the heater holding substrates was spinning with 20 rev/min to make sure that we get uniform thin films on glass substrates.

2.2 Characterization Techniques

Structural properties of prepared thin films were characterized using X-ray diffractometer (XRD), (Unisance S300) equipped with a graphitic monochromator of Cu K α radiation ($\lambda=0.154056$ nm) over the 2θ scan range of 20-70°. To study the surface morphology and optical properties of samples, field emission scanning electron microscope (FESEM), (Hitachi s.4160) and UV-Vis optical spectrometer (300-1100 nm), (Shimadzu UV-Vis 1800) equipment were utilized, respectively.

3. Results and Discussion

3.1. XRD analysis

Fig. 1 shows the X-ray diffraction (XRD) patterns of undoped and tin doped MoO₃ thin films deposited on glass substrates by spray pyrolysis method. The XRD pattern of the undoped sample shows the polycrystalline nature with orthorhombic (α -MoO₃) crys-

tal structure with lattice parameters of $a=3.9620$ Å, $b=13.8580$ Å, $c=3.6970$ Å (according to JCPDS card No. 005-0508). The strong intensity of the reflection peaks of (0 4 0) and (0 6 0) proves the existence of the lamellar structure [4]. Also, Fig. 1 Exhibits that Sn doping of MoO₃ caused attenuation of strong α -MoO₃ peaks, and this continues with increasing in the amount of impurity. However, no peaks have been observed corresponding to the formation of secondary phase regarding SnO₂. Just for the sample with the highest percentage of doping (i.e. Sn/Mo = 0.5), a weak peak of (2 0 2) was observed which can be attributed to the preliminary formation of orthorhombic crystal structure for SnO₂ (according to JCPDS card No. 029-1484). This may be because of atomic substitution of Sn in Mo sites for low concentrations of impurity and beginning the formation of second phase of SnO₂ at high concentrations of doping.

The crystallite size (D (nm)) of prepared thin films was assessed using the famous Scherrer formula [6]:

$$D = \frac{S\lambda}{\beta \cos \theta} \quad (1)$$

where S is the shape factor (~ 0.9), λ is the wavelength of X-rays (1.5406 Å), β (rad) is the full width at half maxima (FWHM), and θ is the diffracting angle (rad). Also, the strain (ε (no dimension)) and dislocation density (δ (nm)⁻²) of the crystallites determined using the following formulas:

$$\varepsilon = \frac{\beta \cos \theta}{4} \quad (2)$$

$$\delta = \frac{1}{D^2} \quad (3)$$

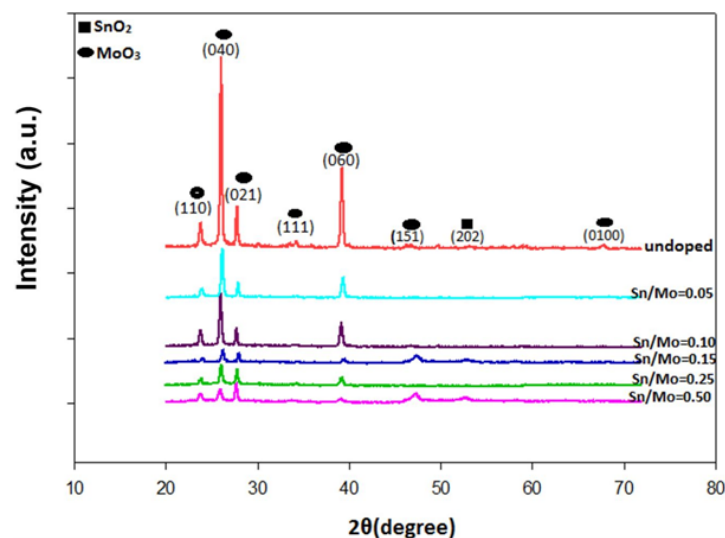


Fig. 1. XRD patterns of undoped and 5, 10, 15, 25 and 50 at% Sn doped MoO₃ thin films.

The crystallite size, strain and dislocation density of crystallites corresponding to the (0 4 0) plane for all samples were calculated and presented in Table 1. Analysis of the data indicates that with increasing the amount of impurity concentration in the precursor solution the crystallite size decreased from about 78 to 23 nm, for undoped and the highly tin doped (Sn/Mo = 0.50) samples, respectively. Also, doping intensification caused increasing the strain and dislocation density of crystallites, which this confirms degradation in crystal quality. This result is also in correlation with FESEM images of samples.

3.2 Surface morphology

In order to observe the surface morphology changes of samples due to the addition of impurities, field emission scanning electron microscopy (FESEM) of thin films were utilized. Before imaging all samples were coated with a thin layer of Au, using DC sputter

coater in order to get clear and high contrast pictures. Fig. 2 shows the FESEM images of undoped and tin doped MoO₃ thin films prepared by spray pyrolysis method. Fig. 2(a) reveals that for undoped sample FESEM images show the formation of some dispersed micro-spheres on the surface. Insets of Fig. 2(a) shows that shell of every micro-sphere has been composed of stacked thin layers and the sphere has been filled by semi-rectangular nano-platelets. Figures 2 (b) - (d) show the surface morphology of tin doped MoO₃ samples with 5, 25 and 50 at% of impurity, respectively. Increasing the dopant amount causes formation of nucleation sites on every platelets and then creation of rectangular nano-plates which can be attributed to the formation of the new SnO₂ orthorhombic crystal structure which is formerly confirmed by XRD pattern analysis.

3.3 Optical properties

The optical properties of all samples were stud-

Table 1.

The crystallite size (D), FWHM (β), strain (ϵ) and dislocation density (δ) of undoped and 5,10,15,25 and 50 at% tin MoO₃ thin films along (0 4 0) plane.

sample	FWHM ($\times 10^{-3}$ rad)	D(nm)	ϵ ($\times 10^{-4}$)	δ ($\times 10^{-4}$ (nm) ⁻²)
Undoped	1.7898	78.88	4.35	1.60
Sn/Mo=0.05	1.9850	71.71	4.83	1.94
Sn/Mo=0.10	2.0925	68.00	5.09	2.16
Sn/Mo=0.15	4.1933	33.95	10.21	8.67
Sn/Mo=0.25	4.6786	30.41	11.39	10.80
Sn/Mo=0.50	6.1200	23.24	14.91	18.50

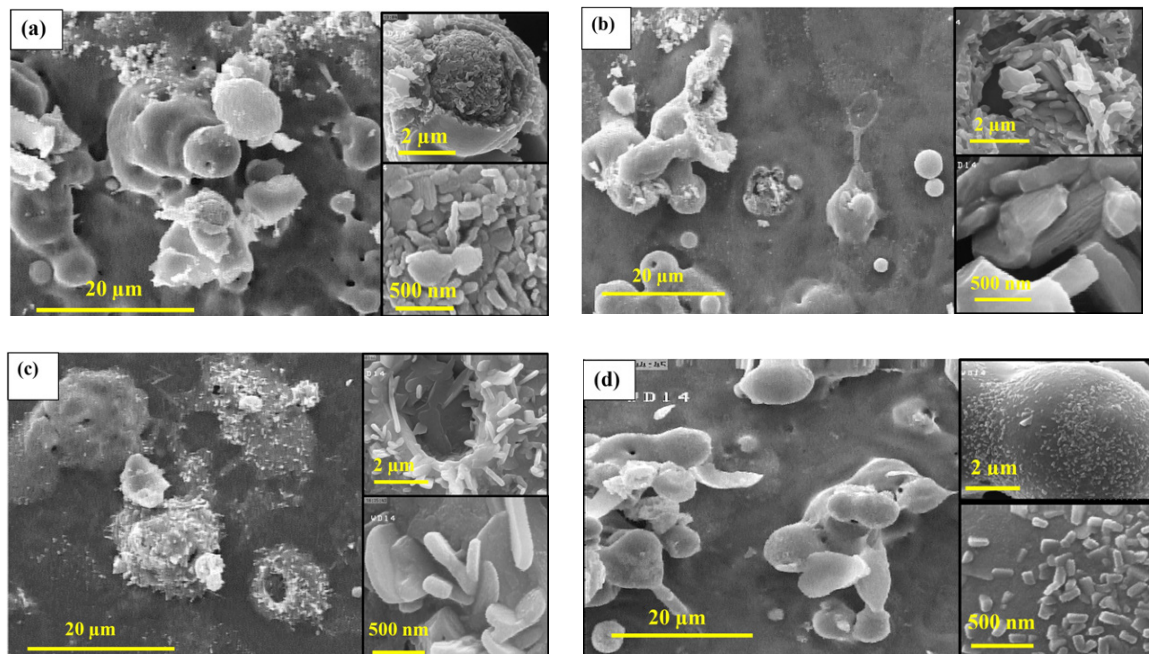


Fig. 2. FESEM images of: (a) undoped, (b) 5, (c) 25 and (d) 50 at% tin doped MoO₃ thin films

ied in the wavelength range of 300 -1100 nm. Fig. 3 shows the optical transmittance spectra of thin films on glass substrates and indicates that the transmittance has increased from about 28 to 51% (in the average wavelength of visible region, i.e. 550 nm), with increasing the percentage of tin as dopant from 0 to 50 at% in precursor solution, respectively. This causes the shift of absorption edges toward lower wavelengths, and can be attributed to the occupation of all states close to the conduction band and the optical band gap increases with increasing the doping amount of Sn according to Burstein-Moss effect [23].

The optical band gap of thin films was obtained by extrapolating of linear region of the curve $(\alpha h\nu)^2$ versus photon energy ($h\nu$) as shown in Fig. 4. Optical band gaps of samples are given in Table 2. The results indicate that the optical band gap increased with increasing the percentage of tin doping and is in agreement with the changes in the crystallite size. Besides Burstein-Moss effect on band gap broadening, the well-known quantum confinement phenomenon causes the increase of band gap by decreasing the crystallite size when the percentage of dopant rises [6].

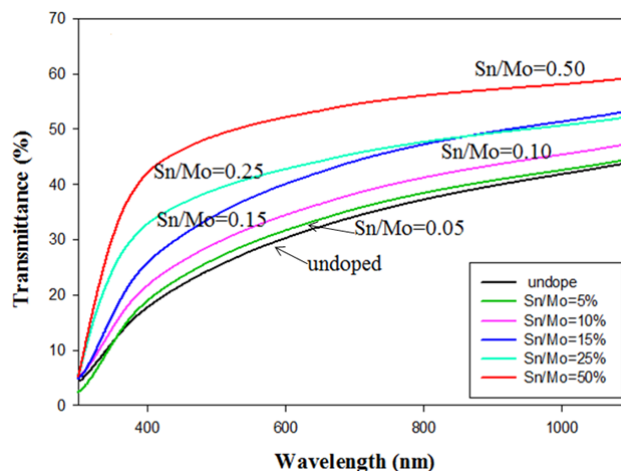


Fig. 3. The optical transmittance spectra of undoped and 5, 10, 15, 25 and 50 at% tin doped MoO_3 thin films.

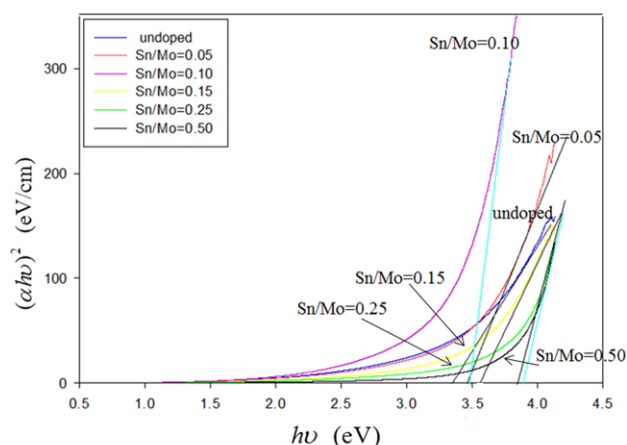


Fig. 4. $(\alpha h\nu)^2$ vs. photon energy ($h\nu$) for undoped and 5, 10, 15, 25 and 50 at% tin doped MoO_3 thin films.

Table 2. Optical band gap and transmittance of undoped and 5, 10, 15, 25 and 50 at% tin doped MoO_3 thin films.

sample	Band gap (eV)	Transmittance (%)
Undoped	3.34	27
Sn/Mo=0.05	3.47	29
Sn/Mo=0.10	3.48	32
Sn/Mo=0.15	3.56	38
Sn/Mo=0.25	3.84	41
Sn/Mo=0.50	3.89	51

4. Conclusions

In this work, we have studied the effect of Sn as a dopant on structural and optical properties of MoO₃ thin films deposited on glass substrates at 450 °C, using the simple and cost effective route of spray pyrolysis. XRD pattern analysis revealed that undoped samples have polycrystalline nature with α -MoO₃ orthorhombic phase which has lamellar (2D) structure. Only one peak was observed for the highly Sn doped MoO₃ thin films, which corresponds to the formation of new second phase of SnO₂ with orthorhombic lattice structure and other samples with lower percentages of impurity just show decreasing in the intensity of MoO₃ main peaks, which is due to incorporation of Sn in Mo sites. The measured transmittance spectra in the average wavelength of 550 nm for samples increased from about 28 to 51% with increasing in the percentage of tin dopant from 0 to 50 at% in precursor solution, respectively. Also, same increasing was observed in the calculated band gap of samples, which was 3.34 to 3.89 eV for samples from 0 to 50% impurity, respectively.

References

- [1] K.-K. Wang, F.-X. Wang, Y.-D. Liu, G.-B. Pan, Vapor growth and photoconductive property of single-crystalline MoO₃ nanosheets, *Mater. Lett.*, 102–103 (2013) 8-11.
- [2] S. Balakumar, R.A. Rakesh, A.K. Prasad, S. Dash, A.K. Tyagi, Nanoplatelet Structures of MoO₃ for H₂ Gas Sensors, *IEEE*, (2011) 514-517.
- [3] M.C. Rao, K. Ravindranadh, A. Kasturi, M.S. Shekhawat, Structural Stoichiometry and Phase Transitions of MoO₃ Thin Films for Solid State Microbatteries, *Res. J. Recent Sci.*, 2(4) (2013) 67-73.
- [4] M.B. Rahmani, S.H. Keshmiri, J.Yu, A.Z. Sadek, L. Al-Mashat, A. Moafi, K. Latham, Y.X. Lie, W. Wlodarski, K. Kalantar-zadeh, Gas sensing properties of thermally evaporated lamellar MoO₃, *Sens. Actuators, B*, 145 (2010) 13-19.
- [5] H.M. Martínez, J. Torres, L.D.L. Carreño, M.E. Rodríguez-García, Effect of the substrate temperature on the physical properties of molybdenum tri-oxide thin films obtained through the spray pyrolysis technique, *Mater. Charact.*, 75 (2013) 184 - 193.
- [6] J. Li, X. Liu, Preparation and characterization of α -MoO₃ nanobelt and its application in supercapacitor, *Materials Letters* 112 (2013) 39-42.
- [7] B. Kannan, R. Pandeewari, B.G. Jeyaprakash, Influence of precursor solution volume on the properties of spray deposited α -MoO₃ thin film, *Ceram. Int.*, 40 (2014) 5817-5823.
- [8] H. Sinaim, A. Phuruangrat, S. Thongtem, T. Thongtem, Synthesis and characterization of heterostructured Ag nanoparticles MoO₃ nanobelts composites, *Mater. Chem. Phys.*, 132 (2012) 358-363.
- [9] S.-Y. Lin, C.-M. Wang, K.-S. Kao, Y.-C. Chen, C.-C. Liu, Electrochromic properties of MoO₃ thin films derived by a sol-gel process, *J. Sol-Gel Sci. Technol.*, 53 (2010) 51-58.
- [10] G. Wang, T. Jiu, P. Li, J. Li, C. Sun, F. Lu, J. Fang, Preparation and characterization of MoO₃ hole-injection layer for organic solar cell fabrication and optimization, *Sol. Energy Mater. Sol. Cells*, 120 (2014) 603-609.
- [11] H.W. Choi, N.D. Theodore, T.L. Alford, ZnO–Ag–MoO₃ transparent composite electrode for ITO-free, PEDOT: PSS-free bulk-heterojunction organic solar cells, *Sol. Energy Mater. Sol. Cells*, 117 (2013) 446-450.
- [12] R. Sivakumar, R. Gopalakrishnan, M. Jayachandran, C. Sanjeeviraja, Characterization on electron beam evaporated α -MoO₃ thin films by the influence of substrate temperature, *Curr. Appl. Phys.*, 7 (2007) 51-59.
- [13] M. Kovendhan, D.P. Joseph, P. Manimuthu, S. Sambasivam, S.N. Karthick, K. Vijayarangamuthu, A. Sendilkumar, K. Asokan, H.J. Kim, B.C. Choi, C. Venkateswaran, R. Mohan, 'Li' doping induced physicochemical property modifications of MoO₃ thin film, *Appl. Surf. Sci.*, 284 (2013) 624-633.
- [14] A.A. Firooz, T. Hyodo, A.R. Mahjoub, A.A. Khodadadi, Y. Shimizu, Synthesis and gas-sensing properties of nano- and meso-porous MoO₃-doped SnO₂, *Sens. Actuators, B*, 147 (2010) 554-560.
- [15] P. Tyagi, A. Sharma, M. Tomar, V. Gupta, Metal oxide catalyst assisted SnO₂ thin film based SO₂ gas sensor, *Sens. Actuators, B*, 224 (2016) 282-289.
- [16] V. Galstyan, E. Comini, C. Baratto, G. Faglia, G. Sberveglieri, Nanostructured ZnO chemical gas sensors, *Ceram. Int.*, 41 (2015) 14239-14244.
- [17] L.-l. Sui, Y.-M. Xu, X.-F. Zhang, X.-L. Cheng, S. Gao, H. Zhao, Z. Cai, L.-H. Huo, Construction of three-dimensional flower-like α -MoO₃ with hierarchical structure for highly selective triethylamine sensor, *Sens. Actuators, B*, 208 (2015) 406-414.
- [18] S.S. Mahajan, S.H. Mujawar, P.S. Shinde, A.I. Inamdhar, P.S. Patil, Structural, optical and electrochromic properties of Nb-doped MoO₃ thin film, *Appl. Surf. Sci.*, 254 (2008) 5895-5898.
- [19] J. Kaur, V.D. Vankar, M.C. Bhatnagar, Effect of MoO₃ addition on the NO₂ sensing properties of SnO₂ thin film, *Sens. Actuators, B*, 133 (2008) 650-655.
- [20] M.M.Y.A. Alsaif, M.R. Field, T. Daeneke, A.F.

- Chrimes, W. Zhang, B.J. Carey, K.J. Berean, S. Walia, J. van Embden, B. Zhang, K. Latham, K. Kalantar-zadeh, J.Z. Ou, Exfoliation Solvent Dependent Plasmon Resonances in Two-Dimensional Sub-Stoichiometric Molybdenum Oxide Nanoflakes, *ACS Applied Materials & Interfaces*, 8 (2016) 3482-3493.
- [21] S. Balendhran, S. Walia, M. Alsaif, E.P. Nguyen, J.Z. Ou, S. Zhuiykov, S. Sriram, M. Bhaskaran, K. Kalantar-zadeh, Field Effect Biosensing Platform Based on 2D α -MoO₃, *ACS Nano*, 7 (2013) 9753-9760.
- [22] M.M.Y.A. Alsaif, A.F. Chrimes, T. Daeneke, S. Balendhran, D.O. Bellisario, Y. Son, M.R. Field, W. Zhang, H. Nili, E.P. Nguyen, K. Latham, J. van Embden, M.S. Strano, J.Z. Ou, K. Kalantar-zadeh, High-Performance Field Effect Transistors Using Electronic Inks of 2D Molybdenum Oxide Nanoflakes, *Adv. Func. Mater.*, 26 (2016) 91-100.
- [23] A.H. Omran Alkhayatt, S.K. Hussian, Fluorine highly doped nanocrystalline SnO₂ thin films prepared by SPD technique, *Mater. Lett.*, 155 (2015) 109-113.

